International Journal of Microwave and Wireless Technologies, 2011, 3(3), 259–266.
doi:10.1017/S1759078711000468

RESEARCH PAPER

Implementation of wideband digital beam forming in the E-band

VAL DYADYUK, XIAOJING HUANG, LEIGH STOKES AND JOSEPH PATHIKULANGARA

This paper reports the test results of a small-scale prototype that implements a digitally beam-formed phased antenna array in the E-band. A four-channel dual-conversion receive RF module for 71–76 GHz frequency band has been developed and integrated with a linear end-fire antenna array. Wideband frequency-domain angle-of-arrival estimation and beam-forming algorithms were developed and implemented using Orthogonal Frequency Division Multiplexing (OFDM) with Quadrature Phase-Shift Keying (QPSK) at 1 Gbps. Measured performance is very close to the simulated results and experimental data for an analogue-beam-formed array. This work is a stepping stone toward practical realization of larger hybrid arrays in the E-band.

Keywords: Active array antennas and components, Hybrid and multi-chip modules, Millimeter-wave radio communication

Received 15 October 2010; Revised 9 March 2011; first published online 19 April 2011

I. INTRODUCTION

High-data-rate millimeter-wave communication systems are of growing importance to the wireless industry. Future mobile and *ad hoc* communications networks will require higher bandwidth and longer range. An *ad hoc* or mobile (e.g. inter-aircraft) network that relies on high-gain antennas also requires beam scanning. With the advance in digital signal processing techniques, the adaptive antenna array is becoming an essential part of wireless communications systems. The use of adaptive antenna arrays for long-range millimeter-wave *ad hoc* communication networks is particularly critical due to increased free space loss and reduced level of practically achievable output power [1]. Although pure digital beam forming (DBF) allows for producing output signals with the maximum Signal-to-Interference and Noise Ratio (SINR), ease of on-line calibration, and generation of many antenna patterns simultaneously, it is impractical for large wideband arrays due to two major reasons. Firstly, it is too costly since the cost of digital data processing is proportional to bandwidth and increases, at least, linearly with the number of elements. Secondly, the small separation of array elements in the E-band (71–86 GHz) leaves little room at the back of the array for connection of each RF chain associated with individual array elements to a digital beam former. A typical analogue RF chain is tightly packed behind each antenna element and includes a low-noise amplifier (or power amplifier), frequency converter, local oscillator (LO), as well as the intermediate frequency (IF) or baseband circuitry. Each of these chains would require a number of DC, IF, and control circuit interfaces. Therefore, a hybrid approach [1–3] where DBF technique is applied to a smaller number of units (analogue beam formed sub-arrays) is preferable. This provides a significant saving both in the amount of digital signal processing and the number of physical connections between the RF front end and digital beam former. A small scale E-band phased antenna array has been developed [1] for an experimental verification of the hybrid beam-forming concepts [2, 3]. Analogue beam forming (ABF) of this array using 6-bit phase shifters and attenuators at IF has been reported earlier in [4, 5]. In this paper, we report the test results of an E-band prototype that implements a DBF phased antenna array.

ICT Centre, Commonwealth Scientific and Industrial Research Organisation (CSIRO), P.O. Box 76, Epping, Sydney, NSW 2121, Australia.
Phone: +61 29372 4225.
Corresponding author:
V. Dyadyuk
Email: val.dyadyuk@csiro.au

II. E-BAND PHASED ANTENNA ARRAY PROTOTYPE

The prototype has been developed to demonstrate a communications system with gigabit per second data rates using an electronically steerable array as an initial step toward fully ad hoc communications systems. The prototype configuration is flexible and can be used for experimental verification of both analogue and DBF algorithms. Figure 1 shows the equipment configuration for DBF experiments. The steerable receive array is mounted on a rotator providing mechanical steering in the azimuth plane for the array-pattern measurement.

IF to baseband frequency conversion was implemented in the receive (Rx IF) and transmit (Tx IF) IF modules. The Rx IF module has been developed in two versions. For DBF, each of the IF analogue signals was digitized and streamed to a PC for data processing and beam forming as shown in Fig. 2. For ABF [4, 5], the phase and magnitude of each channel were controlled by 6-bit phase shifters and attenuators and a

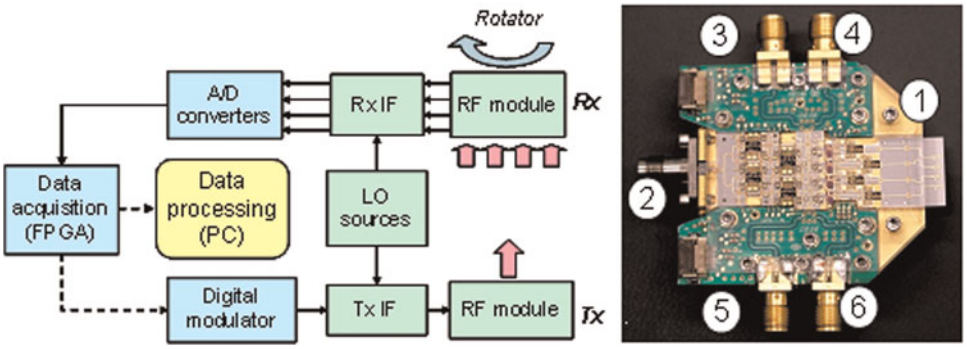

Fig. 1. (a) Block diagram of the test setup; (b) photograph of the RF module assembly where 1 is the antenna array, 2 is the LO input, and 3–6 are IF outputs.

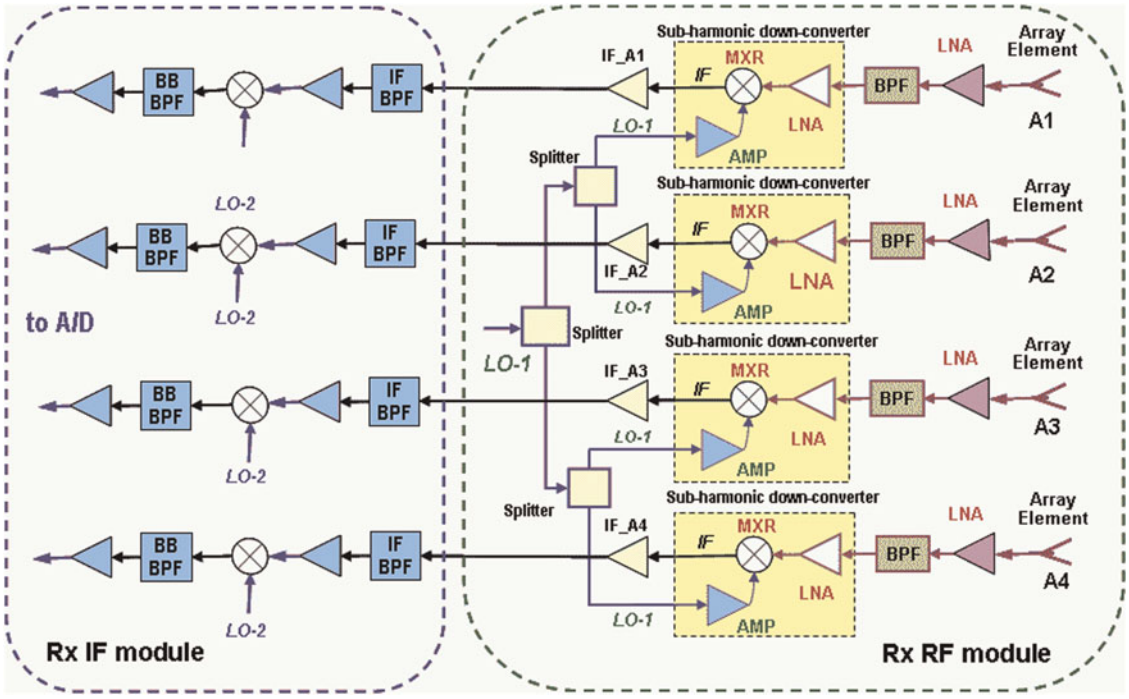

Fig. 2. Block diagram of the receiver configured for DBF experiments.

combined IF signal was de-modulated using a modem reported in [6]. This replaces the digitizer shown in Fig. 1(a) for the DBF configuration. The demonstrator also includes a digital modulator reported in [6] and a single-channel transmitter [1].

The transmit module has been built using the up-converter [7], a commercial low-pass filter, a medium power amplifier, and a corrugated horn antenna. Bench test results have been reported in [1]. The main functional block of the prototype is a four-channel receive RF module [1, 4] integrated with a linear end-fire quasi-Yagi antenna array [5, 8]. Array element spacing was 2 mm (or 0.48 wavelengths at the carrier frequency) to suppress appearance of grating lobes for scanning angles up to $\pm 42^{\circ}$. The RF module uses sub-harmonic frequency converters at the LO frequency of 38 GHz. For each channel we have used a combination of CSIRO's and commercial off-the-shelf Monolithic Microwave Integrated Circuits (MMICs) similar to those reported earlier for a single-channel receiver [7, 9]. The IF pre-amplifiers, interconnecting, matching, and group delay equalization circuits have been developed using a standard commercial thin-film process on

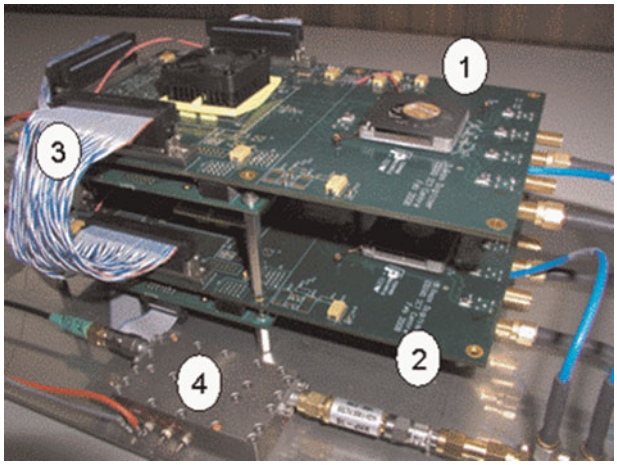

Fig. 3. Photograph of the digitizer module assembly where 1 and 2 are two identical digitizers, 3 is interconnecting cable, and 4 is a sampling oscillator.

https://doi.org/10.1017/S1759078711000468 Published online by Cambridge University Press

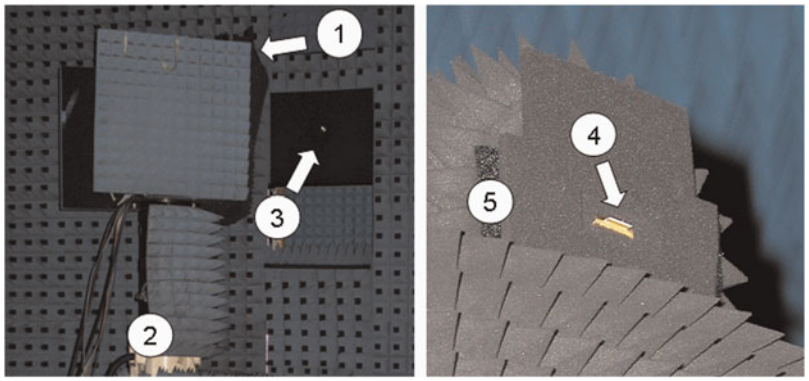

Fig. 4. System test setup in the 12 m far-field anechoic chamber where 1 is the receive array RF module, 2 is the rotator and 3 is the transmit antenna aperture, 4 is the receive antenna array masked with absorbers 5.

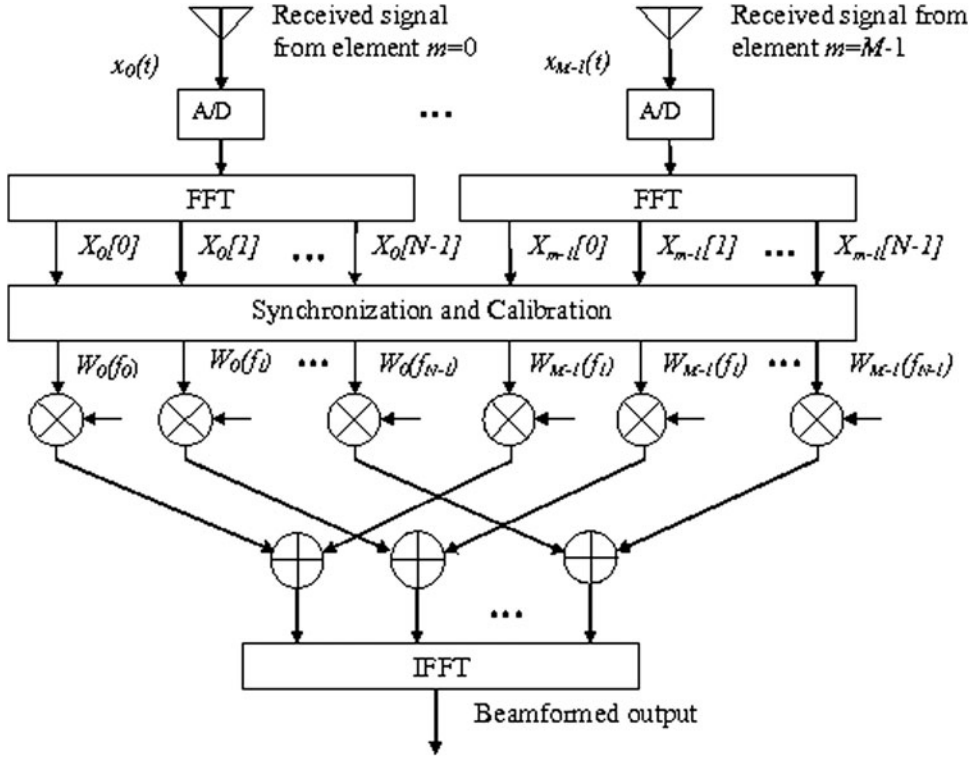

Fig. 5. Frequency-domain digital beam former structure.

ceramic substrate. Figure 1(b) shows a photograph of the assembled RF module. It includes 16 MMICs, 12 types of microwave boards (on 127 μm alumina substrate), 140 microwave passives, and about 400 wire-bond connections. The receiver is usable over the frequency range of 71–76 GHz at the sub-harmonic LO of 38–39 GHz and IF 1–7 GHz. Typical conversion gain was 6 ± 1 dB over the operating RF and IF frequency range of 71.5–72.5 and 3.5–4.5 GHz, respectively. The maximum magnitude imbalance between each of the four channels was below ±1.5 dB. Bench test results for the receive module have been reported in [1]. The IF to baseband (1–2 GHz) frequency conversion was implemented in the Rx IF module [5].

The digitizer consists of an analogue-to-digital converter (ADC) and a field programmable gate array (FPGA). The ADC is an EV8AQ160 (E2V Semiconductors) 8-bit device. This converter is used in dual-channel mode, each channel sampling at 2 Giga samples per second [10]. The ADC has an effective number of bits (ENOB) of 6 bits at the frequency of operation and input bandwidth of 2 GHz. The FPGA for

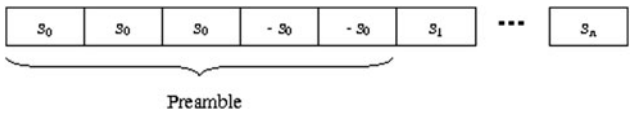

Fig. 6. Transmitted signal format.

https://doi.org/10.1017/S1759078711000468 Published online by Cambridge University Press

signal processing is a Xilinx V5SX95T. The experimental setup uses two such digitizers as shown in Fig. 3 giving a total of four ADCs and two FPGAs. The interconnections labeled "3" in the photograph of Fig. 2 have enough bandwidth to transport digital signals after pre-processing on one FPGA to the other for DBF. In this experiment, the samples are captured on the FPGA internal memory and uploaded to a PC for processing.

All measurements were conducted in the CSIRO 12 m far-field anechoic chamber as shown in Fig. 4. Transmitter, digital modulator, and control equipment were located on the outside of the chamber. The available signal-to-noise ratio was above 33 dB for the measurement distance up to 6 m, but most of the tests were conducted at the distance of 2.2 m to minimize unwanted reflections from the walls and ceiling of the chamber.

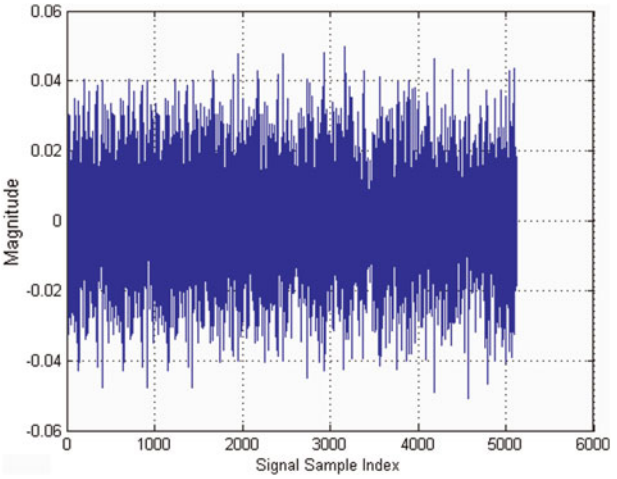

Fig. 7. Transmitted digital IF signal.

III. DBF ALGORITHM

A) Received signal model

Consider a linear wideband array with M elements and element spacing d. Denoting the received baseband signal from the mth element as $x_m(t)$, the frequency-domain model of the received signal can be expressed as

$$X_m(f) = S(f)H_m(f)P(f,\theta)e^{j[(f+f_c)/f_c](2\pi/\lambda_c)dm\sin\theta} + Z_m(f), \quad \text{for } |f| \le \frac{B}{2}, \quad m = 0, 1, \ldots, M-1, \tag{1}$$

where $X_m(f)$ is the Fourier transform of $x_m(t)$, $S(f)$ is the information-bearing reference signal in the frequency domain, $H_m(f)$ is the channel frequency response of the RF chain for the mth element, $P(f,\theta)$ is the element radiation pattern, f_c and λ_c are the frequency and wavelength of the RF carrier, respectively, $Z_m(f)$ is zero-mean complex Gaussian noise, and B is the bandwidth of the signal.

For digital implementation, the received time-domain signals $x_m(t)$, $m = 0,1, \ldots, M-1$, are sampled at $t = nT$, that is, $x_m[n] = x_m(nT)$ is the received signal sequence from the mth element, where $T = 1/B$ is the sampling period, and divided into blocks of size N. Each block is converted into the frequency domain by fast Fourier transform (FFT). The discrete model is then expressed as

$$X_m[k] = S[k]H_m[k]P(f_k,\theta)e^{j[(f_k+f_c)/f_c](2\pi/\lambda_c)dm\sin\theta} + Z_m[k], \quad \text{for } k = 0, 1, \ldots, N-1, \tag{2}$$

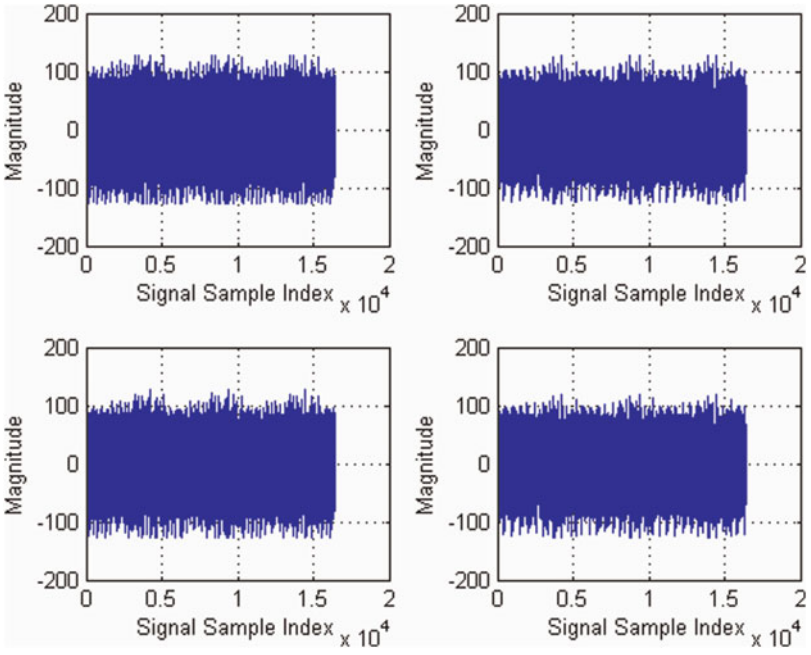

Fig. 8. Captured four-channel received signals at 0° azimuth.

https://doi.org/10.1017/S1759078711000468 Published online by Cambridge University Press

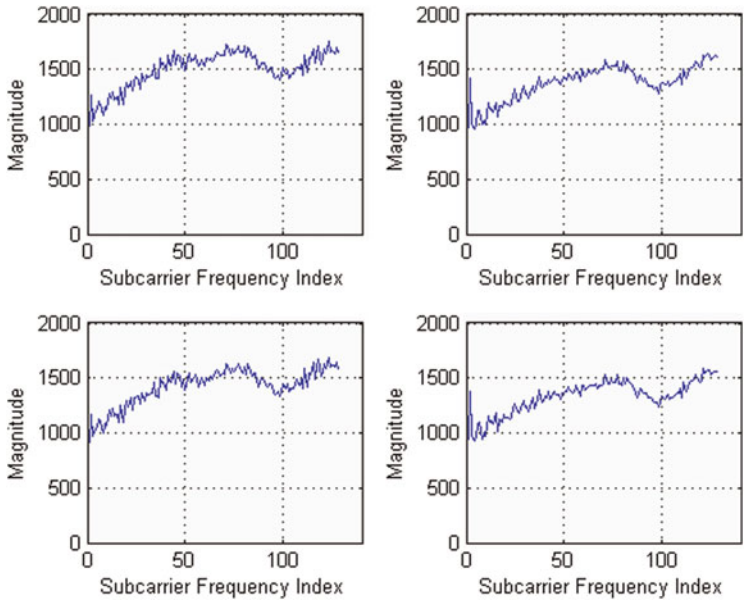

Fig. 9. Magnitude frequency response for each channel o° azimuth.

where the index k represents a discrete frequency

$$f_k = \begin{cases} \dfrac{kB}{N}, & \text{for } k = 0, 1, \ldots, \dfrac{N}{2} - 1, \\ \dfrac{(k-N)B}{N}, & \text{for } k = \dfrac{N}{2}, \dfrac{N}{2} + 1, \ldots, N - 1, \end{cases} \tag{3}$$

X_m [k], $S[k]$, $H_m[k]$, and Z_m[k] are the mth received frequency-domain signal, reference signal, frequency response, and noise at discrete frequency f_k, respectively.

B) Frequency domain beam forming

In order to achieve maximized signal-to-noise ratio, the frequency-domain DBF is performed as follows. First, the signal sequence received at each element is synchronized, and the combined channel frequency response together with the phase shift introduced by the incident angle (i.e., $H_m[k]$ $P(f_k, \theta)e^{j[(f_k+f_c)/f_c](2\pi/\lambda_c)dm\sin\theta}$ as a whole) is estimated using the training sequence during the preamble period. Then, the synchronized signal after the preamble is converted into the frequency domain by FFT, and the channel frequency response at each discrete frequency is compensated by the inverse of the channel frequency response. Finally, the

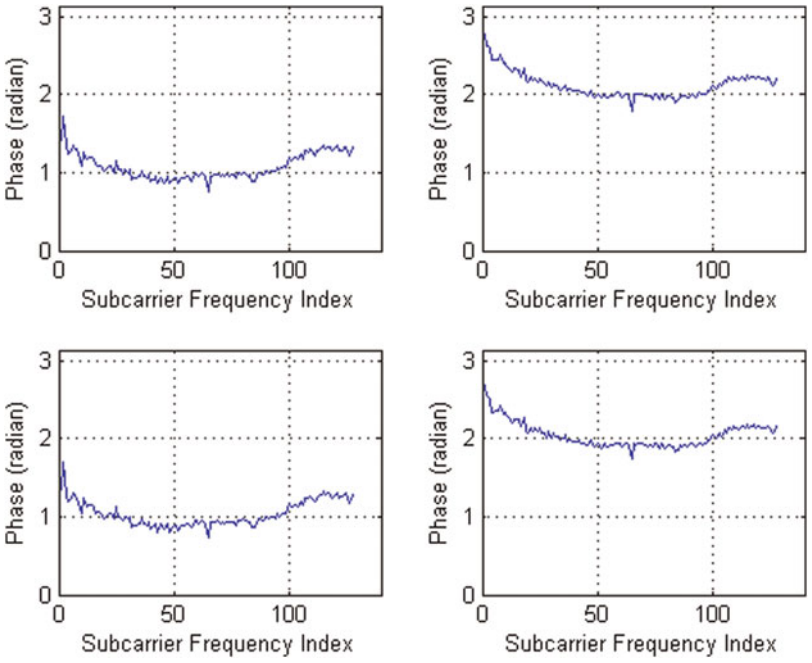

Fig. 10. Phase frequency response for each channel o° azimuth.

https://doi.org/10.1017/S1759078711000468 Published online by Cambridge University Press

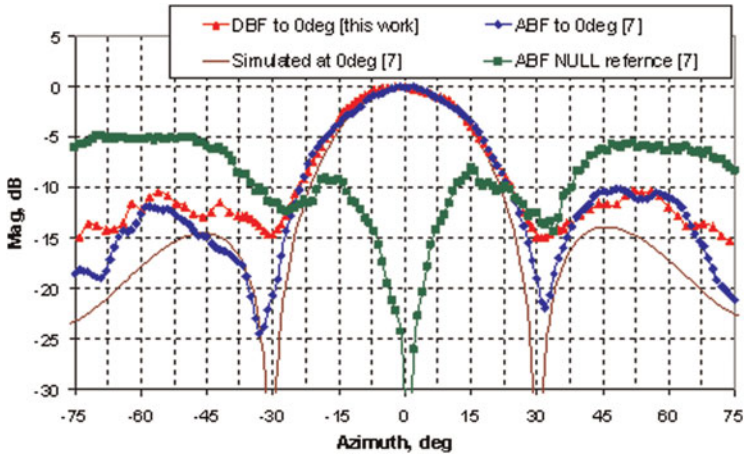

Fig. 11. Comparison of the *E*-plane co-polar radiation patterns for DBF and ABF array [5] at 0° azimuth.

compensated frequency-domain signals for all elements are summed up and the combined signal is converted into time domain by inverse FFT (IFFT).

To obtain the angle-of-arrival (AoA) information or form a beam for a specified incident angle, the receiver array needs to be calibrated. This calibration can be done for each element after compensation of the channel frequency response $H_m[k]$ only. $H_m[k]$ can be estimated in advance from the signal preamble received at 0° incident angle for each element.

The frequency-domain beam forming at a specified incident angle is performed as follows. First, the signal sequence received at each element is synchronized using the preamble. Then, the synchronized signal after the preamble is converted into the frequency domain by FFT followed by calibration. After calibration, the frequency-domain signals are weighted with coefficients

$$W_m(f_k) = e^{-j[(f_k+f_c)/f_c](2\pi/\lambda_c)\,dm\sin\theta_o}, \tag{4}$$

where θ_o is the incident angle at which a beam is to be formed. The weighted signals are finally summed up and converted into the time domain by IFFT to obtain the beam-formed output signal. The structure of this frequency-domain digital beam former is shown in Fig. 5.

IV. TEST RESULTS

The DBF experiments were conducted by transmitting a 1 Gbps OFDM test signal with $N = 128$ sub-carriers used in the $B = 0.5$ GHz bandwidth. QPSK is used for data modulation. To facilitate synchronization and channel estimation, a preamble composed of five predefined OFDM symbols is pre-pended before the information bearing reference sequence. The signal format is shown in Fig. 6, where s_0 denotes the predefined training sequence and $s_1, \ldots, s_n$ denote the reference sequence composed of n OFDM symbols with pseudo-random data modulated by QPSK.

To reduce hardware cost as well as overcome the practical impairments involved in frequency conversion, such as the in-phase (I) and quadrature phase (Q) vectors (!/Q) imbalance, the received RF signal is first converted into IF signal with center frequency 1.5 GHz and thus only one ADC operating

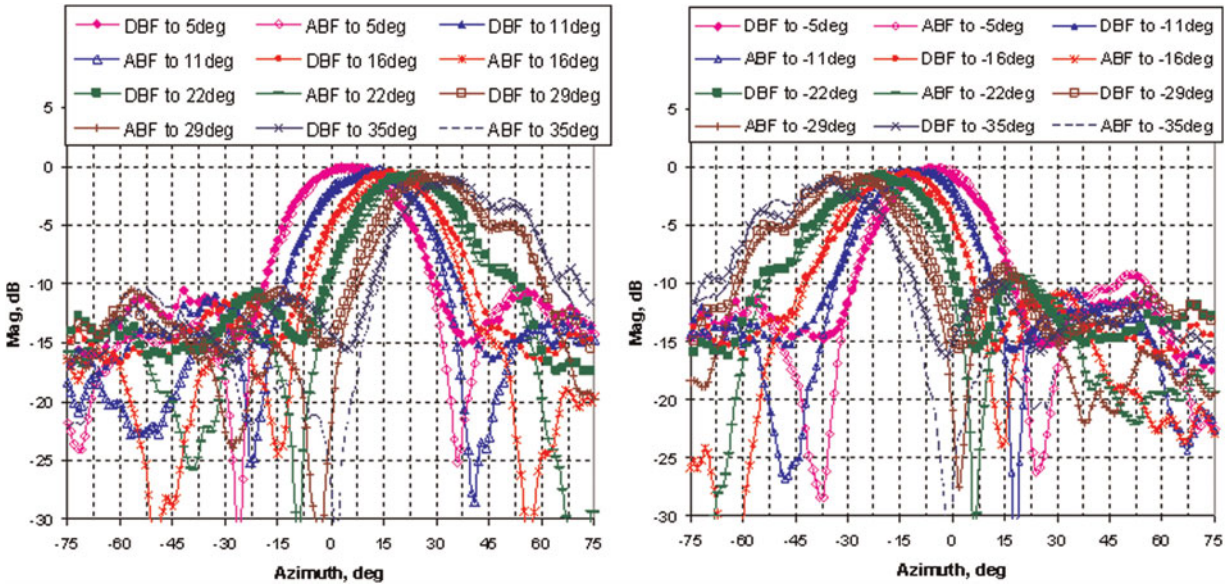

Fig. 12. E-plane co-polar radiation patterns for DBF and analogue beam-formed ABF array [5] for a selection of positive and negative azimuth angles.

https://doi.org/10.1017/S1759078711000468 Published online by Cambridge University Press

at 2 GHz is necessary. Each OFDM symbol has 512 samples in the time domain after A/D conversion at IF. The digital complex baseband signal is then obtained through digital down-conversion. The receive array was rotated in the azimuth plane from -75 to 75° in 1° step. For each azimuth angle the received signals were digitized, captured on the FPGA internal memory, uploaded to a PC and processed as described in Section III.B. Figure 7 shows the transmitted digital IF signal with 5120 samples. The first five OFDM symbols form the preamble, followed by five random reference symbols. The received signals from the four channels in the array with incident angle 0°, each having 16384 samples, are captured at the receiver FPGA after A/D conversion, which are shown in Fig. 8.

After synchronization, channel estimation is performed for each channel using the fifth OFDM symbol in the preamble. The magnitude frequency response and phase frequency response for each channel are shown in Figs 9 and 10, respectively. The phases (represented as complex numbers) averaged over 128 sub-carriers for the four channels are calculated as $0.4773 + j0.8787$, $-0.5120 + j0.8590$, $0.5087 + j0.8610$, and $-0.4503 + j0.8929$, respectively, which are used for calibration.

A separate ABF experiment was also conducted at selected incident angles using the same antenna array for comparison and verification of the DBF results. Figure 11 compares the *E*-plane co-polar array radiation patterns at 0° azimuth computed by the DBF and measured for the ABF [5]. In both experiments the calibration was performed at 0° azimuth angle. For the ABF [5], the array has been calibrated by canceling the main beam to obtain a null at 0° azimuth. The null ABF calibration reference is also shown in Fig. 11.

The *E*-plane co-polar radiation patterns of the DBF array for a selection of other positive and negative azimuth angles are shown in Fig. 12 with the magnitude normalized to the maximum of the main beam at 0° azimuth angle.

Measured *E*-plane co-polar radiation patterns for the ABF array [5] are appended to the computed DBF results shown in Fig. 12. Measured array gain was 9.5 dBi for steering angles below 11° and reduced to approximately 8.4 dBi at the steering angle of $\pm 35^\circ$. Obtained DBF results were in a very close agreement with those measured for the ABF array and EM simulation predictions [5] for steering angles within $\pm 40^\circ$. The magnitude and angle of the DBF and ABF main beam patterns were within 1 dB and 1°, respectively. Beam steering accuracy of 1° has been achieved by both DBF and ABF methods.

V. CONCLUSION

A steerable E-band receive array demonstrator that implements a four-element linear antenna array has been tested using a wideband frequency-domain DBF algorithm. Obtained DBF array patterns were very close to those measured for the analogue beam-formed array and EM-simulated predictions. Beam steering accuracy of 1° has been achieved for steering angles within $\pm 40^\circ$. Demonstrated wideband adaptive DBF along with validated phase-only ABF at IF can be used for hybrid beam forming of larger arrays. To our knowledge, this work represents the first experimental results on the digitally beam-formed antenna array in the E-band.

REFERENCES

[1] Dyadyuk, V.; Guo, Y.J.: Towards multi-gigabit ad-hoc wireless networks in the E-band, in Global Symp. on Millimeter Waves (GSMM2009), Sendai, Japan, 2009.

[2] Huang, X.; Guo, Y.J.; Bunton, J.D.: A hybrid adaptive antenna array. IEEE Tran. Wirel. Commun. **9** (5) (2010), 1770–1779.

[3] Huang, X.; Guo, Y.J.; Bunton, J.D.: Adaptive AoA estimation and beamforming with hybrid antenna arrays, in IEEE VTC-Fall, Alaska, USA, 2009.

[4] Dyadyuk, V.; Stokes, L.: Wideband adaptive beam forming in the E-band: towards a hybrid array, in Global Symp. on Millimeter Waves, Incheon, Korea, 2010.

[5] Dyadyuk, V.; Stokes, L.; Nikolic, N.; Weily, A.R.: Demonstration of adaptive analogue beam forming in the E-band. J. Korean Inst. Electromagn. Eng. Sci., **10** (3) (2010), 138–145.

[6] Dyadyuk, V.; Bunton, J.D.; Pathikulangara, J. et al.: A multi-gigabit mm-wave communication system with improved spectral efficiency. IEEE Trans. Microw. Theory Tech., **55** (12 Part 2) (2007), 2813–2821.

[7] Dyadyuk, V.; Stokes, L.; Shen, M.: Integrated W-band GaAs MMIC modules for multi-gigabit wireless communication systems, in Global Symp. on Millimeter Waves, Nanjing, China, 2008.

[8] Deal, W.R.; Kaneda, N.; Sor, J.; Qian, Q.Y.; Itoh, T.: A new quasi-Yagi antenna for planar active antenna arrays. IEEE Trans. Microw. Theory Tech. **48** (6) (2000), 910–918.

[9] Dyadyuk, V.; Archer, J.W.; Stokes, L.: W-Band GaAs Schottky diode MMIC mixers for multi-gigabit wireless communications, in Agbinya, J. I. et al., eds. Advances in Broadband Communication and Networks, River Publishers, Denmark, 2008, 73–103.

[10] Dyadyuk, V.; Huang, X.; Stokes, L.; Pathikulangara, J.: Implementation of wideband digital beam forming in the E-band: towards a hybrid array, in The 40th European Microwave Conf. (EuMC2010), Paris, France, 2010, 914–917.

Val Dyadyuk received B.Sc. and M.Sc. degrees in electrical engineering in 1968 and 1970, respectively, from Kharkov Institute for Radio Electronics in Ukraine. He is currently the research team leader in Microwave Systems at CSIRO ICT Centre, Sydney. Previously, he held positions of the Head of the Microwave Engineering Branch at Institute for Radio Physics and Electronics, NASU, Ukraine, and Director of Research at the SCAD Scientific & Industrial Group (Kharkov, Ukraine). Mr. Dyadyuk is a recipient of the Engineers Australia (Sydney Division) R&D Excellence Award 2007, and a joint recipient of the CSIRO Chairman's Medal 2007, and the Australian Engineering Excellence Award 2007 for exceptional research in gigabit wireless communications. He has published three book chapters and over 40 journal and conference papers, and holds 10 patents. His research interests include millimeter-wave wireless communication systems, EM simulations and design of GaAs and InP MMICs, and various microwave circuits.

https://doi.org/10.1017/S1759078711000468 Published online by Cambridge University Press

Xiaojing Huang received his bachelor of engineering, master of engineering, and Ph.D. in electronic engineering degrees from Shanghai Jiao Tong University, China, in 1983, 1986, and 1989, respectively. From 1989 to 1994, Dr. Huang worked in the Electronic Engineering Department of Shanghai Jiao Tong University as a Lecturer since 1989 and an Associate Professor since 1991. From 1994 to 1997 he was the Chief Engineer with Shanghai Yang Tian Science and Technology Corporation Limited, China. From 1998 to 2003, he was a Senior and Principal Research Engineer at Motorola Australian Research Centre in Sydney. From 2004 to 2009, Dr. Huang was an Associate Professor in the School of Electrical, Computer and Telecommunications Engineering, University of Wollongong, Australia. In March, 2009, he joined the CSIRO ICT Centre, Australia, as a Principal Research Scientist. His research interests are in communications theory, digital signal processing, and wireless communications networks.

Leigh Stokes received a B.A. degree in economics from Macquarie University, Sydney, Australia in 1978, electronics engineering certificate from North Sydney TAFE in 1988, and postgraduate certificate in project management from University of Technology, Sydney, Australia in 2003. He was the Principal Technical Officer in charge of maintenance (1992–1998) at Waverley Radio Terminal, for Telstra in Sydney, which housed digital radio links. He joined the CSIRO ICT Centre, Sydney, Australia in 2002. Mr. Stokes is the Manager for the GHz Testing Facility for millimeter-wave measurements including on-wafer probing of MMICs. He is also responsible for integration of the research prototypes, test setup, and development of software for automated measurements. Mr. Stokes is a joint recipient of a Millimeter-Wave Best Paper Award from the 9th Topical Symposium on Millimeter Waves (TSMMW 2007) and a joint recipient of CSIRO Chairman's Medal in 2007 for exceptional research in gigabit wireless communications.

Joseph Pathikulangara received a B.E. degree in electronics and communication engineering from Indian Institute of Science in 1984 and M.Tech degree in computer science and engineering from IIT, Bombay in 1991. He was with the Defense Research and Development Organization in India developing command, control and communication systems for missile and EW projects between 1984 and 1995. Since joining CSIRO in Sydney, Australia in 1995, he has been developing signal processors and software radios in various forms for several application spaces. He is responsible in developing specialist expertise in leading edge digital techniques, signal processing and FPGA technologies and maintaining flexible and configurable building blocks that can be rapidly adapted to provide quick engineering solutions. Mr. Pathikulangara is a joint recipient of CSIRO Chairman's Medal in 2007 for exceptional research in gigabit wireless communications.

https://doi.org/10.1017/S1759078711000468 Published online by Cambridge University Press